Site-directed mutagenesis reveals the interplay between stability, structure, and enzymatic activity in RidA from *Capra hircus*

Giulia Rizzi[1], Stefania Digiovanni[1], Genny Degani[1], Alberto Barbiroli[2], Flavio Di Pisa[3], Laura Popolo[1], Cristina Visentin[1]*, Maria Antonietta Vanoni[1], Stefano Ricagno[1, 4]*

[1] Dipartimento di Bioscienze, Università degli Studi di Milano, Via Giovanni Celoria, 26, 20133, Milan, Italy

[2] Dipartimento di Scienze per gli Alimenti, la Nutrizione e l'Ambiente, Università degli Studi di Milano, Via Celoria, 2, 20133, Milan, Italy

[3] Istituto di Biofisica, Consiglio Nazionale delle Ricerche, Via Alfonso Corti, 12, 20133, Milan, Italy

[4] Institute of Molecular and Translational Cardiology, I.R.C.C.S. Policlinico San Donato, Piazza Malan, 2, 20097, San Donato Milanese, Italy

* Corresponding authors:

Cristina Visentin: cristina.visentin@unimi.it

Stefano Ricagno: stefano.ricagno@unimi.it

Running title: RidA mutations to study protein stability and function.

Manuscript: 16 pages.

Supplementary material: 7 pages.

Tables: 1. Figures: 4

All Supplementary materials are reported in one file named “231123_Rizzi_et_al_suppl” and contains:

- Figure S1. Far-UV CD spectra of $_{Ch}$RidA variants (A), human and plant RidA (B) recorded at 25 °C.
- Table S1. Catalytic efficiency of $_{Ch}$RidA variants towards different imino acid substrates.
- Table S2. X-ray diffraction data collected on single crystals. The PDB code and the refinement statistics are listed.
- Table S3. Root mean square deviations obtained from the superposition of mutant trimers to the wild type $_{Ch}$RidA.
- Table S4. Conditions employed for the crystallization of each $_{Ch}$RidA variant.
- Detailed Material and methods for the structural determination of $_{Ch}$RidA-R107K, $_{Ch}$RidA-V25W, and $_{Ch}$RidA-I126Y.

ABSTRACT

Reactive intermediate deaminase A (RidA) is a highly conserved enzyme that catalyses the hydrolysis of 2-imino acids to the corresponding 2-keto acids and ammonia. RidA thus prevents the accumulation of such potentially harmful compounds in the cell, as exemplified by its role in the degradation of 2-aminoacrylate, formed during the metabolism of cysteine and serine, catalysing the conversion of its stable 2-iminopyruvate tautomer into pyruvate. *Capra hircus* (goat) RidA ($_{Ch}$RidA) was the first mammalian RidA to be isolated and described. It has the typical homotrimeric fold of the Rid superfamily, characterised by remarkably high thermal stability, with three active sites located at the interface between adjacent subunits. $_{Ch}$RidA exhibits a broad substrate specificity with a preference for 2-iminopyruvate and other 2-imino acids derived from amino acids with non-polar non-bulky side chains. Here we report a biophysical and biochemical characterisation of eight $_{Ch}$RidA variants obtained by site-directed mutagenesis to gain insight into the role of specific residues in protein stability and catalytic activity. Each mutant was produced in *Escherichia coli* cells, purified and characterised in terms of quaternary structure, thermal stability and substrate specificity. The results are rationalised in the context of the high-resolution structures obtained by X-ray crystallography.

KEYWORDS

RidA, reactive intermediate deaminase A, metabolic damage, 2-aminoacrylate, 2-imino acids, X-ray crystallography, protein stability

50-75-WORD STATEMENT

RidA is an evolutionary conserved enzyme essential for cell fitness. This study uses a protein engineering approach to analyze the features responsible for stability, enzymatic activity and

their relationships. The high-resolution structures revealed local fine differences that highlighted the unexpected role of specific residues although the homotrimeric structure of the protein variants was not affected, consistently with the robustness of this family of enzymes.

ABBREVIATIONS AND SYMBOLS

RidA: Reactive intermediate deaminase A

$_{Ch}$RidA: *Capra hircus* RidA

wt: wild-type

CD: circular dichroism

SEC-MALS: size exclusion chromatography - multi angle light scattering

rmsd: root mean square deviations

2-IP: 2-iminopyruvate

2-AA: 2-aminoacrylate

INTRODUCTION

Reactive intermediate deaminase A (RidA) are small proteins conserved in all domains of life, and part of the YjgF/YER057c/UK114 protein superfamily[1]. Their functional role has been largely debated. It has been recently reported that human RidA (HRSP12) could have a role in promoting the endoribonucleolytic cleavage of some transcripts[2,3], but only the deaminase activity has been demonstrated to be physiologically relevant so far[1]. These enzymes accelerate the conversion of imino acids (a harmful product of amino acid metabolism) to the final products ammonia and 2-keto acids[4,5]. In particular, they are active against the imine derived from the oxidation of α-amino acids, by L- or D- amino acid oxidases, and have been proposed to participate in the degradation of 2-aminoacrylate (2-AA)[6] through hydrolysis of its stable 2-iminopyruvate (2-IP) tautomer. 2-AA is produced by serine/threonine dehydratase and by cysteine desulfhydrase, but its accumulation is associated with decreased cell fitness and alteration of metabolic pathways[7,8]. Cellular toxicity associated with 2-AA accumulation is likely ascribed to the irreversible inactivation of pyridoxal-5'-phosphate-dependent enzymes mediated by 2-AA or 2-IP[6,9]. RidA proteins are attracting increasing attention as they belong to the diverse and growing class of enzymes that protect the cell from damages, caused by reactive metabolites that are physiologically produced in the cell, or that repair damaged intermediates[10].

The first mammalian RidA was identified in the perchloric acid-soluble extract of *Capra hircus* (goat) liver ($_{Ch}$RidA). It was referred to as UK114 or Prp14, and it was one of the founding members of the YjgF/YER057c/UK114 structural family. The early studies focused on its antigenic properties[11]. More recently, following the seminal work of Lambrecht *et al.*[12], it was demonstrated to be also a *bona fide* RidA[13]. Like all RidA that have been structurally characterized, it is a homotrimer with a chorismate mutase-like fold[14]. The active site is nestled between adjacent subunits, as shown by the structures of complexes with pyruvate[15]

and 2-ketobutyrate[16]. In particular, Arg107 (*C. hircus* numbering, Arg165 in *Arabidopsis thaliana* and Arg105 in *Escherichia coli*) was reported to be essential for the catalytic activity by binding the α-carboxylate group of the 2-imino acid substrate in the active site [12].

$_{Ch}$RidA was the first RidA to be systematically investigated with respect to its substrate specificity *in vitro*, revealing a preference for small and aliphatic imino acids, compared to bulky and aromatic ones, and lack of activity with those carrying a charged side-chain[13]. Besides its acid-stability, which was attributed to the lack of ionizable and polar residues in the core of the protein[17], another property of $_{Ch}$RidA is its remarkably high thermal stability, with a half-life of heat inactivation at 95 °C of 3.5 h[13]. This exceptional stability has been proposed to be involved in the capability of this protein to induce a strong immunomodulatory response[13].

Specific residues involved in the stability of the trimeric assembly have been identified in *Arabidopsis thaliana* RidA ($_{At}$RidA) using a site-directed mutagenesis approach[15]. Such study showed that the salt bridge between Lys136 and Glu182 (Lys78 and Glu124 in *C. hircus* numbering, respectively) of two facing monomers is important for stabilization of the oligomeric assembly, and its disruption leads to partial trimer dissociation. The H-bond between the side chain of Ser80 and the backbone nitrogen of Ser162, and that between Ser92 and Arg165 were also reported to further stabilize the trimeric conformation[15]. A similar approach was used to study human RidA ($_{Hs}$RidA) with partially contrasting results with respect to those obtained with the $_{At}$RidA. Arg107 substitutions were found to lead to loss of activity and trimer stability, whereas the disruption of the intermolecular salt bridge did not alter protein stability[18]. The same study identified Asp93, Tyr21 and Phe89 as residues crucial for the enzymatic activity, in addition to Arg107[18].

Beyond its role in imine metabolism, RidA has been proposed to have several effects on human health. Firstly, Der f 34, the RidA homologue of *Dermatophagoides* spp., appears to

be responsible for house dust mite allergy[19]. Furthermore, $_{Hs}$RidA dysregulation, as well as post-translational modification[20], has been associated with tumour development[21–24]. These different effects may be related to the unique biophysical properties of this protein.

In this work we used a protein engineering approach to establish the role of different protein regions with respect to $_{Ch}$RidA fold stability, trimeric assembly, and enzymatic activity. All the protein variants were produced in *E. coli* and biophysically characterized. Their substrate specificity and crystallographic structures were determined. The data reported here show unexpected effects of the amino acid substitutions on the RidA structural and functional properties. $_{Ch}$RidA displays an exceptionally resilient structure; through mutation its enzymatic activity could be negatively and positively tuned and, interestingly, new substrate specificities could be identified. These properties suggest that $_{Ch}$RidA may be a promising protein scaffold for biotechnological enzymatic evolution.

RESULTS

Design of $_{Ch}$RidA mutants

RidA proteins are ubiquitous and well conserved in all kingdoms of life as shown in Figure 1A, reporting the alignment of the amino acid sequences of representative RidA. All RidA orthologues are small proteins with an average of 137 residues (Fig. 1A) resulting in a monomer with a chorismate mutase-like fold that assembles in homotrimers (Fig. 1B and C). *A. thaliana* RidA has an N-terminal extension to target the protein to the chloroplast. The multiple alignment highlights that most of the RidA sequence is either conserved or conservatively substituted across the kingdoms of life (Fig. 1A), as previously reported[7,13,25]. To better understand the molecular determinants of the unique conformational stability of $_{Ch}$RidA[13], eight single amino acid substitutions were designed (Fig. 1C). All the selected residues are fully or almost fully conserved along evolution stressing their pivotal role in

RidA proteins[7,13,25]. The first set of mutations targeted residue Arg107. This arginine residue has been proposed to be essential for catalysis since it would bind the imino acid substrate by interacting with the α-carboxylic group and favour imine hydrolysis by promoting the postulated nucleophilic addition of a water-derived hydroxyl group onto the adjacent alpha C[15]. In addition, this residue has been reported to play a role in maintaining the stability of $_{Hs}$RidA[18]. Arg107 was substituted with Ala ($_{Ch}$RidA-R107A) to disrupt the catalytic activity, with Lys ($_{Ch}$RidA-R107K) to modify the position of the positive charge, and with Trp ($_{Ch}$RidA-R107W) that is found in members of the Rid4 and Rid7 families, and maintains a bulky side chain as well as the possibility to form H-bonds with the substrate[7]. A second set of RidA variants was designed to disrupt the unique salt bridge between two facing monomers to test whether its removal affects protein assembly, as observed in $_{At}$RidA, or leaves the trimer intact, as observed for $_{Hs}$RidA[15,18]. To this aim, Lys78 and Glu124 were individually substituted with Ala residues ($_{Ch}$RidA-K78A and $_{Ch}$RidA-E124A). Finally, three positions, at the interface between RidA subunits (Val25, Ala108, Ile126) were substituted with chemically different amino acids to assess their impact on trimer stability and catalytic activity. Thus, the $_{Ch}$RidA-V25W, $_{Ch}$RidA-A108D and $_{Ch}$RidA-I126Y variants were designed.

Protein expression and biophysical characterisation

The $_{Hs}$RidA, $_{At}$RidA-68S and all $_{Ch}$RidA variants were expressed in *E. coli* and purified at homogeneity according to a previously established protocol[13]. In $_{At}$RidA, a truncated protein was expressed according to Liu *et al.*[15] to remove the N-terminal sequence corresponding to the signal peptide targeting the protein to the chloroplast. The oligomeric state and the molecular mass in solution of all proteins were assessed. Our analyses estimated a molecular mass of 43.8 kDa for wild-type (wt) $_{Ch}$RidA (Table 1), in good agreement with what reported

by Degani *et al.*[13]. SEC and SEC-MALS analyses indicate that all RidA variants showed almost identical mass to that of the wt $_{Ch}$RidA thus all are trimeric in solution (Table 1). The effect of amino acid substitutions on the secondary structure content of RidA forms was evaluated by far-UV circular dichroism (CD) analysis as reported in Figure S1. For comparison the CD spectra of $_{Hs}$RidA and $_{At}$RidA-68S were also collected, confirming that all RidA variants had a CD spectrum typical for RidA family members. This indicates that the substitutions did not significantly alter the protein's secondary structure.

Then, protein thermal stability was determined by recording the CD ellipticity at 220 nm upon temperature increase from 30 to 98 °C. Due to the exceptional stability of wt $_{Ch}$RidA, no unfolding event was observed in such temperature range, preventing the calculation of a melting temperature (T_m) in keeping with previous reports[13]. Similar results were obtained for $_{Hs}$RidA, $_{Ch}$RidA-R107A, $_{Ch}$RidA-R107K, $_{Ch}$RidA-R107W, $_{Ch}$RidA-K78A, and $_{Ch}$RidA-E124A variants in which no loss of secondary structure was detected. Conversely, for $_{At}$RidA-68S, $_{Ch}$RidA-A108D, $_{Ch}$RidA-I126Y, and $_{Ch}$RidA-V25W variants, protein unfolding was observed, leading to the calculation of melting temperatures of 82 °C, 87 °C, 86 °C and 70 °C, respectively (Table 1).

To better differentiate the stability of RidA variants, the experiments were repeated in presence of 4M urea. This specific urea concentration was selected based on data reported by Degani *et al.*[13], which showed a linear dependence of $_{Ch}$RidA unfolding and urea concentration. Under these experimental conditions a T_m value could be determined for wt $_{Ch}$RidA, for $_{Ch}$RidA interface mutants (except $_{Ch}$RidA-K78A) and for the human and plant RidA (Table 1). These experiments confirmed that amino acid substitutions involving interfaces residues were destabilizing but to different extent: from marginal effect of the A108D substitution, to a mild effect of the E124A and I126Y to the big impact of the V25W

substitution. Interestingly both $_{Hs}$RidA, and $_{At}$RidA-68S showed a significant decrease in T_m suggesting a lower stability compared to $_{Ch}$RidA.

Unexpectedly, the mutations of the catalytic residue R107 and K78A led to further stabilisation of the $_{Ch}$RidA fold and protein unfolding could not be observed under these conditions (Table 1).

Effect of mutations on enzymatic activity

RidA family members catalyse the hydrolysis of α-imino acids, which can be generated *in situ* by the action of L-amino acid oxidase from the corresponding L-amino acid and molecular oxygen to yield the imino acid and hydrogen peroxide[4]. The activity assay exploits the rapid spontaneous reaction of the imino acid released by the oxidase with semicarbazide to yield the corresponding semicarbazone, which can be continuously monitored spectrophotometrically from the absorbance increase at 248 nm. RidA causes a decrease of the rate of formation of the semicarbazone so that its catalytic efficiency with the different imino acids can be determined from the estimate of the concentration of RidA that halves the velocity of semicarbazone formation that is observed in its absence (K_{50}). It has been shown that $100/K_{50}$ is a measure of such catalytic efficiency[13].

The activity of $_{Ch}$RidA and its engineered variants was measured in the presence of a selected series of imino acids representing various amino/imino acid classes (Fig. 2). All assays were carried out at 25°C where all enzyme forms are fully folded.

Substitution of Arg107 with an alanine residue led to complete loss of activity with all imino acids tested (Fig. 2 and Table S1), as expected with its proposed role to ion pair with the substrate α-carboxylate group[16]. A virtually complete loss of activity was also observed in the $_{Ch}$RidA-R107K variant, despite the presence of a positively charged group. Surprisingly, the $_{Ch}$RidA-R107W retained some activity, which was, however, always less than 10% that measured with the wt enzyme with the same imino acid. Two-three-fold decrease of catalytic

efficiency was observed for $_{Ch}$RidA-K78A and $_{Ch}$RidA-E124A variants, with 2-IP remaining the best substrate. Unexpectedly, substituting Ala108, the residue adjacent to Arg107, with an aspartate residue caused the same loss of activity as that observed with the R107A substitution. The I126Y substitution targeting the interface between adjacent subunits of the RidA trimer caused an almost negligible effect on the specific activity of the enzyme with 2-IP (<10% decrease of catalytic efficiency), an approximately 2-fold decrease of activity with the L-leucine derivative and a 3-4-fold decrease with the other imino acids tested.

The V25W substitution led to a ~30% decrease of activity with 2-IP, but a ~50% increase of activity with the imino acid derived from L-leucine. Surprisingly, the Val-to-Trp substitution also caused a ~50% gain of activity with the imino acid derived from L-Glu, a ~30% and ~250% increase of the catalytic efficiency with the imino acids derived from L-Trp (indolpyruvate) and L-Phe (phenylpyruvate), respectively. Unique to this variant, activity with the L-His derivative was observed, which remained – however – very low compared to that measured with 2-keto acids (Fig. 2).

Impact of mutations on protein structure

Crystal structures of all $_{Ch}$RidA variants were determined at high resolution by X-ray crystallography (Table S2) and confirmed the homotrimeric assembly typical of the RidA proteins (Table 1). Each subunit exhibited the chorismate mutase-like fold, characterised by a six-stranded β-sheet packed against two α-helices (Fig. 3B).

To evaluate the structural effects brought about by the amino acid substitutions, the structures of the protein variants were superimposed and compared with the previously reported structure of wt $_{Ch}$RidA (PDB: 1NQ3) (Fig. 3 and Table 3). The root mean square deviation (rmsd) obtained from trimer superposition suggests that the structures of $_{Ch}$RidA variants

closely match that of wt $_{Ch}$RidA (Table S3), confirming the high degree of secondary structure similarity among all variants previously shown by CD data.

In all structures, high-quality electron density was visible for the amino acid substitution site and surrounding residues. Analysis of the three mutants of the catalytic residue Arg107 (R107A, R107K, R107W) revealed that, regardless of the different chemical properties of the side chain, residue 107 always showed a similar orientation (Fig. 4A-C).

In the $_{Ch}$RidA-R107K mutant, the conformation of Lys107 was extended and well superposed on the Arg107 side chain of the wt protein (Fig. 4B). In the $_{Ch}$RidA-R107W mutant, the secondary amine NE1 of Trp was oriented comparably to the secondary amine NE-HE of wt Arg107, which has been reported to interact with the negatively charged α-carboxylic group (Fig. 4C)[16]. While the conformation of Arg107 remained substantially unchanged, the orientation of surrounding residues varied significantly, depending on the nature of the side chain at position 107. In presence of bulky amino acids at position 107, i. e., Lys and Trp, the surroundings were virtually identical to the wt structure (Fig 4B-C). On the contrary, in the $_{Ch}$RidA-R107A mutant, Tyr21 side chain flipped filling the region occupied by the guanidinium group of Arg107 in wt $_{Ch}$RidA. As a consequence, the whole 15-21 loop facing the active site moved inwards, sealing the access to the protein active site (Fig 4A).

The $_{Ch}$RidA-E124A and $_{Ch}$RidA-K78A, which were designed to prevent the formation of the intermolecular salt bridge E124-K78, did not show any specific local rearrangement with respect to the native protein, both exhibiting a 3D structure perfectly superposable to that of wt $_{Ch}$RidA (Fig 4D-F).

The three single V25W, A108D and I126Y substitutions targeted three residues at the trimeric interface. Although in all cases the wt residue was substituted with a residue carrying a bulkier side chain, with potential disruptive effects, the trimeric assembly was not perturbed in any of the mutants. Nevertheless, each of the three substitutions contributed significantly

to the reduced $_{Ch}$RidA fold stability as detected with thermal denaturation in 4 M urea (Table 1).

Val25 is located on β2 strand with the side chain pointing towards β6 strand of the adjacent subunit (Fig. 4G), and it is in the middle of a highly hydrophobic patch at the interface between subunits. Although substitution of Val residue with the bulkier Trp had no impact on protein secondary structure and Trp hydrophobicity is chemically compatible with that of the pocket, it results in a reorientation of the adjacent secondary structures, including the loop between α2 and β5 strand and β2 strand, to accommodate Trp25 (Fig. 4G).

Although residue Ala108 is adjacent to the catalytic Arg107, its side chain is not oriented towards the active site but rather towards the neighbouring subunit of the trimer (Fig. 4H). Ala108 is surrounded by two negatively charged residues: Glu122, pointing into the active site cleft, and Glu124, involved in the intermolecular salt bridge with Lys78, as mentioned above. Thus, the A108D substitution increases the local concentration of negative charges. In this $_{Ch}$RidA variant a novel intramolecular salt bridge between Asp108 and Lys78 is formed, substituting the Glu124-Lys78 salt bridge present in the wt protein. Moreover, a slight movement of the Glu122 side chain towards the active site cavity, and in particular towards Arg107, was observed. Overall, the $_{Ch}$RidA fold well accommodates this Ala-to-Asp substitution in an interface region, in keeping with the marginal effect observed on thermal stability (Table 1).

Ile126 lies far from the active site but extends into the trimer central cavity. Although Ile-to-Tyr substitution did not trigger any major side chain rearrangement, three bulky Tyr are now located at the trimer interface in very close proximity (Fig 4I).

DISCUSSION

RidA is part of YjgF/YER057c/UK114 protein superfamily[1], and catalyses the hydrolysis of 2-IP to pyruvate to prevent the hazardous accumulation of 2-AA, its less stable tautomer released by serine dehydratase and cysteine desulfydrase. $_{Ch}$RidA is the first characterized mammalian member of the RidA family. It displays a deiminase activity with a preference for small and aliphatic imino acids, and it is characterized by a remarkably high thermal stability[13]. We applied a rational engineering approach to deepen our understanding of $_{Ch}$RidA as a protein and as an enzyme.

Three groups of amino acid substitutions were designed to target: i) the catalytic residue ($_{Ch}$RidA-R107A, $_{Ch}$RidA-R107K, and $_{Ch}$RidA-R107W); ii) the intermolecular salt bridge ($_{Ch}$RidA-K78A, and $_{Ch}$RidA-E124A) and iii) the inter-subunit interface ($_{Ch}$RidA-V25W, $_{Ch}$RidA-A108D and $_{Ch}$RidA-I126Y). These residues were chosen because they are highly conserved in RidA proteins (they are either conserved or only conservative substitutions are found) and/or because of their position within the protein (Val25, Ala108, and Ile126) (Fig. 1A and 1C). All the protein variants were successfully expressed in a soluble form and purified with yields similar to those of the wt protein. The amino acid substitutions did not alter the homotrimeric assembly of RidA (Table 1), and all the protein variants maintained the typical RidA secondary structure footprint, as shown by CD spectroscopy (Fig. S1).

In agreement with the exceptional stability of the $_{Ch}$RidA scaffold, most of its variants display minor or no changes in thermal stability under native conditions in the tested temperature range (Table 1); thus temperature unfolding was also performed under destabilising conditions (4M Urea).

Overall, none of the mutations disrupts $_{Ch}$RidA trimeric assembly, and only the $_{Ch}$RidA-V25W variant displayed a significantly lower stability compared to the wt protein. These data show that trimeric $_{Ch}$RidA well tolerates both potentially destabilising interface mutations (V25W, A108D and I126Y) and mutations in the active site or in its surroundings (mutants of

Arg107 and A108D). Moreover mutations of an inter-subunit salt bridge that were previously reported to disassemble the trimer in $_{Hs}$RidA[17] and $_{At}$RidA[15] had no effect on $_{Ch}$RidA trimer. The higher fold stability observed for $_{Ch}$RidA compared to the ones of $_{Hs}$RidA and $_{At}$RidA may account for such distinct behaviour.

As expected, the substitutions of the catalytic Arg107 ($_{Ch}$RidA-R107A, $_{Ch}$RidA-R107K, and $_{Ch}$RidA-R107W) heavily affect the RidA enzymatic activity with all the tested substrates. In particular, $_{Ch}$RidA-R107A did not display any enzymatic activity. Although the removal of the positive charge needed to bind the substrate α-carboxylate would be the obvious reason of such loss of activity, the crystallographic model suggests that the imino acid substrate may no longer accesses the active site. Indeed, the small Ala107 side chain allows an inward conformation of 15-21 loop effectively sealing the active site, thus likely reducing the accessibility of active site to substrate molecules (Fig 5A). Compared to $_{Ch}$RidA-R107A, $_{Ch}$RidA-R107K showed a measurable, although low, residual activity, indicating that the positive charge alone is not sufficient to support the activity of the wt enzyme. While in the Rid superfamily the catalytic residue is mainly represented by Arg, Rid4 and Rid7 orthologues present a Trp in the catalytic position, thus a Trp mutant was prepared. The bulkiest mutant ($_{Ch}$RidA-R107W) is the most active of these three variants, maintaining residual activity especially with small substrates (Fig. 2). This observation suggests that the presence of a secondary amine group facing the negative charge of the substrate (present in both the side chains of Arg and Trp) is more important than the presence of a positively charged residue to ensure the enzyme's functionality (Fig. 4C). The crystallographic structure of $_{Ch}$RidA-R107W reveals that larger amino acids at position 107 can be accommodated without significant structural realignment of the active site. Therefore, our data suggests that in $_{Ch}$RidA, Trp is suboptimal catalytic residue and only partial catalytic activity is maintained.

The amino acid substitutions that prevent formation of the intermolecular salt bridge, ($_{Ch}$RidA-K78A and $_{Ch}$RidA-E124A) do not cause any decrease in fold stability nor any detectable structural rearrangement, and yet the corresponding RidA variants exhibit a 2-fold decrease of activity with 2-IP, the preferred imino acid substrate, and a 3-4-fold decrease with the other compounds. Unfortunately, due to the instability of 2-imino acids, it is not possible to distinguish between k_{cat} or K_m effects of the amino acid substitutions. The crystal structures of these variants do not clarify the effects on enzymatic activity caused by these mutations. However, the vicinity of the E124-K78 salt bridge to the active site and the minor rearrangements observed upon its loss may account for the limited changes in enzymatic activity.

Similarly, the $_{Ch}$RidA-A108D variant is very poorly active with all the tested substrates, although the protein is properly folded and assembled into a stable trimer. Introduction of Asp108 next to two other negatively changed residues (namely Glu122 and Glu124) leads to a structural rearrangement in which the Glu122 side chain fills the active site, thus affecting substrate binding and/or proper positioning for catalytic activity. Accordingly, the I126Y substitution, located away from the active site, decreases RidA stability, but it has virtually no effect on the geometry of the active site cavity at the interface between the subunits. The I126Y has unaltered activity with 2-IP, bearing a small side chain, but a 2-3 fold lower activity with the other imino acid substrates, which are all bulkier than 2IP. Here, the lower thermal stability may reflect a higher local flexibility that alters binding and/or proper positioning for catalysis of the imino acid substrates other than the small (and preferred) 2-IP, as previously discussed for the effect of substitutions that abrogated the K78-E124 salt bridge.

The behaviour of $_{Ch}$RidA-V25W variant was unexpected in the light of the position of residue 25 far from the active site, the trimer stability at 25°C and the geometry of the active site

upon V25W substitution. Indeed, $_{Ch}$RidA-V25W enzymatic activity on the Ala and Leu derivatives was similar to that of wt $_{Ch}$RidA but surprisingly, the activity increased with large or charged substrates (imino acids derived from Phe, Trp and Glu). For the first time, a measurable (although low) activity with the L-His derivative was also observed. One possible explanation is that the V25W mutation, which also lays at the inter-subunit interface, may increase the flexibility and adaptability of the active site by reducing the stability of the inter-subunit interface. Alternatively, the substitution at position 25 may affect the behaviour of the 15-21 loop, which acts as a gate of the active site. In the crystallographic structure, the loop is mostly superposable with that of wt RidA, but it cannot be ruled out that - in solution - the loop may populate different conformations. Indeed, in one (out of six) of the monomers present in the crystallographic unit the density of the loop is not well defined, and the average B factor of the loop is higher compared to the wt, suggesting a high flexibility of the region. Even though the present data do not fully elucidate this point, they demonstrate that $_{Ch}$RidA has the potential to acquire new enzymatic activities with potentially very disruptive mutations, which, however, can be accommodated by such a stable trimeric assembly. Thus, unpredictable effects are in play in the intricate relationship between trimeric assembly, fold stability and enzymatic activity in $_{Ch}$RidA.

The deiminase activity of $_{Ch}$RidA, once its activity would be properly optimised, could be used in several different contexts[13,25]. For example, RidA forms with altered substrate specificity could be of interest in mechanistic studies to determine which species is actually released by an imine-generating enzyme. Moreover, it could be used in conjunction with D- or L-AAO to accelerate the formation of 2-keto acids in bioconversion or coupled with aminotransferases to avoid a transient accumulation of imino acids, which can act as aminotransferases inhibitors.

In summary, the ChRidA variants analysed in this work highlight that the striking stability of ChRidA ensures the maintenance of its native trimeric native state in presence of potentially destabilising mutations (trimer interface or active site). The enzymatic activity is preserved or even improved/modified in non-trivial ways. Contrary to expectations, our data showed that a properly positioned secondary amine in the active site is pivotal to stabilise the interaction with the substrate. Moreover, specific mutations surrounding Arg107 or the 15-21 loop could finely tune the enzymatic activity or substrate specificity. Overall, this work shows that ChRidA scaffold has the robustness to well tolerate even non-conservative mutations in different locations. At the same time, the modifications in enzymatic activity observed in ChRidA variants suggest that wt ChRidA active site possesses the evolvability to be a promising starting point to design new enzymatic activities for future biotechnological applications.

MATERIALS AND METHODS

Protein sequence analysis

Protein sequence of RidA from *Salmo salar* (Isoform 1, UniProt KB: A0A1S3KNQ3), *Salmo salar* (Isoform 2, UniProt KB: C0H8I4), *Capra hircus* (UniProt KB: P80601), *Homo sapiens* (UniProt KB: P52758), *Mus musculus* (UniProt KB: P52760), *Oryctolagus cuniculus* (UniProt KB: G1U8R2), and *Escherichia coli* (UniProt KB: P0AF93) were aligned using ClustalOmega[26]. The resulting multi-alignment was analysed and visualised with ESPript 3.0[27].

Protein expression and purification

The DNA sequences coding for human, plant (68S truncated mutant[15]), goat wt and R107A-, R107K-, R107W-, K78A-, E124A, V25W-, A108D-, and I126Y-RidA were codon optimized

for expression in *E. coli* and purchased by GENEWIZ GmbH (Germany) as synthetic genes cloned into a pET15b expression vector. The recombinant proteins carry an N-terminal 6XHis-tag and a thrombin recognition site. All protein forms were produced in *E. coli* Rosetta (DE3) cells and purified as reported in Degani *et al.*[13].

Analytical size exclusion chromatography – multi- angle light scattering.

SEC combined with MALS was performed in a FPLC system equipped with a Wyatt Dawn Multi-Angle Light Scattering MALS (Wyatt Technology, Santa Barbara, CA) detector. A Superdex 75 10/300 GL (Cytiva, USA) column equilibrated with 154 mM NaCl was used to analyse 500 μg of $_{Ch}$RidA variants.

Circular dichroism

Circular dichroism analyses were carried out on a J-1500 spectropolarimeter (JASCO Europe) equipped with a Peltier system for temperature control using a 0.1 cm path length quartz cuvette. $_{Ch}$RidA variants were diluted to 0.2 mg/mL in 154 mM NaCl or 154 mM NaCl, 4 M urea. Far-UV spectra were recorded from 195 to 260 nm at 25°C. The mean residual ellipticity ($[\theta]_{MRW, \lambda}$)[28] is reported. Temperature ramps were recorded from 30 to 98 °C at a heating rate of 1 °C/min while monitoring CD signal at 220 nm. T_m values were determined as the maximum of the first derivative of the unfolding profiles.

RidA enzymatic activity

The activity of RidA forms was assayed at 25°C as previously described by measuring the initial velocity of formation of the semicarbazone derived by the reaction of semicarbazide with the imino acid produced by L-amino acid oxidase in the presence of its L-amino acid substrate and varying concentrations of the RidA form (v_{RidA}) in comparison with the velocity

of the same reaction measured in the absence of RidA (v_o)[25,29]. To avoid artefacts the enzymatic test has been optimised to ensure that LAAO produces all imino acids at the same velocity[13,30].

The percentage residual activity, expressed as v_{RidA}/v_o*100, as a function of RidA concentration was fitted to Eq. 1 to obtain the estimate of the concentration of RidA that halves the v_o value (K_{50}). With the imino-tryptophan substrate, a constant non-zero activity was measured due to slow, but detectable, reaction of the indolpyruvate product with semicarbazide. Thus, Eq. 2, which takes into account such background reaction, was used to fit the data. The $100/K_{50}$ value has been shown to be a measure of the catalytic efficiency (k_{cat}/K_m) of the enzyme with the imino acid being used[13]. When very low RidA activity was observed, the data were fitted with a straight line. The absolute value of the slope is directly the $100/K_{50}$ value, from which K_{50} can be calculated[13,30].

Eq .1 $$v, \% = \frac{100}{1+\frac{[RidA]}{K50}}$$

Eq 2. $$v, \% = \frac{100-B}{1+\frac{[RidA]}{K50}} + B$$

Protein crystallization and structure determination

Purified mutant $_{Ch}$RidA at a typical concentration of 9 mg/ml in 154 mM NaCl was subjected to crystallization trials using an Oryx4 crystallization robot (Douglas Instruments. UK). Crystallization screening experiments were performed in 96-well sitting drop plates, which were incubated at 20 °C. Conditions that led to crystals of diffracting quality are listed in Table S4. Crystals were cryo-protected by adding 25% glycerol and flash-frozen in liquid nitrogen. X-ray diffraction data were collected at cryogenic temperature (100 K) at the European Synchrotron Radiation Facility (ESRF, Grenoble, France) on ID23-2 or ID30-A

beamline equipped with a DECTRIS EIGER X 9M or Eiger X 4M detector, respectively. All structures were determined by molecular replacement by MOLREP[31] using the coordinates of the wt goat protein (PDB: 1NQ3) as search model. Initial molecular replacement solutions were subjected to subsequent cycles of manual building in Coot[32] and refinement with phenix.refine[33]. For $_{Ch}$RidA-R107K, $_{Ch}$RidA-V25W and $_{Ch}$RidA-I126Y a slightly different protocol was used as detailed in Supplementary material. Models were inspected and validated using MolProbity[34]. Processing and refinement statistics are reported in Table S2. The PDB codes obtained by the deposition of the coordinates and structure factors are 8QOQ for $_{Ch}$RidA-R107A, 8QOU for $_{Ch}$RidA-R107K, 8QOM for $_{Ch}$RidA-R107W, 8QOP for $_{Ch}$RidA-K78A, 8QOK for $_{Ch}$RidA-E124A, 8QOS for $_{Ch}$RidA-V25W, 8Q3H for $_{Ch}$RidA-A108D, and 8QOV for $_{Ch}$RidA-I126Y. Structural images were generated using CCP4mg[35].

SUPPLEMENTARY MATERIAL DESCRIPTION

Figure S1. Far-UV CD spectra of $_{Ch}$RidA variants (A), human and plant RidA (B) recorded at 25 °C.

Table S1. Catalytic efficiency of $_{Ch}$RidA variants towards different imino acid substrates.

Table S2. X-ray diffraction data collected on single crystals. The PDB code and the refinement statistics are listed.

Table S3. Root mean square deviations obtained from the superposition of mutant trimers to the wt $_{Ch}$RidA.

Table S4. Conditions employed for the crystallization of each $_{Ch}$RidA variant.

$_{Ch}$RidA-R107K structure determination

$_{Ch}$RidA-V25W structure determination

$_{Ch}$RidA-I126Y structure determination

ACKNOWLEDGMENTS

The work was supported by Fondazione Baggi Sisini to GR, by Ricerca Corrente funding from Italian Ministry of Health to IRCCS Policlinico to SR, by the Italian Ministry of Research and Education (PRIN 20207XLJB2) to SR. Fondazione Umberto Veronesi is gratefully acknowledged for the support to CV. We kindly acknowledge Giovanni Robecchi and Letizia Grillo for technical assistance, and Prof. Alberto Bartorelli and Prof. Saverio Minucci for helpful discussions.

REFERENCES

1. Irons JL, Hodge-Hanson K, Downs DM (2020) RidA Proteins Protect against Metabolic Damage by Reactive Intermediates. Microbiol. Mol. Biol. Rev. MMBR 84:e00024-20.

2. Schmiedeknecht G, Kerkhoff C, Orsó E, Stöhr J, Aslanidis C, Nagy GM, Knuechel R, Schmitz G (1996) Isolation and characterization of a 14.5-kDa trichloroacetic-acid-soluble translational inhibitor protein from human monocytes that is upregulated upon cellular differentiation. Eur. J. Biochem. 242:339–351.

3. Park OH, Ha H, Lee Y, Boo SH, Kwon DH, Song HK, Kim YK (2019) Endoribonucleolytic Cleavage of m6A-Containing RNAs by RNase P/MRP Complex. Mol. Cell 74:494-507.e8.

4. Lambrecht JA, Schmitz GE, Downs DM (2013) RidA proteins prevent metabolic damage inflicted by PLP-dependent dehydratases in all domains of life. mBio 4:e00033-00013.

5. Downs DM, Ernst DC (2015) From microbiology to cancer biology: the Rid protein family prevents cellular damage caused by endogenously generated reactive nitrogen species. Mol. Microbiol. 96:211–219.

6. Borchert AJ, Ernst DC, Downs DM (2019) Reactive Enamines and Imines In Vivo: Lessons from the RidA Paradigm. Trends Biochem. Sci. 44:849–860.

7. Niehaus TD, Gerdes S, Hodge-Hanson K, Zhukov A, Cooper AJL, ElBadawi-Sidhu M, Fiehn O, Downs DM, Hanson AD (2015) Genomic and experimental evidence for multiple metabolic functions in the RidA/YjgF/YER057c/UK114 (Rid) protein family. BMC Genomics 16:382.

8. Borchert AJ, Walejko JM, Guennec AL, Ernst DC, Edison AS, Downs DM (2019) Integrated Metabolomics and Transcriptomics Suggest the Global Metabolic Response to 2-Aminoacrylate Stress in Salmonella enterica. Metabolites 10:E12.

9. Shen W, Borchert AJ, Downs DM (2022) 2-Aminoacrylate stress damages diverse PLP-dependent enzymes in vivo. J. Biol. Chem. 298:101970.

10. Niehaus TD, Nguyen TND, Gidda SK, ElBadawi-Sidhu M, Lambrecht JA, McCarty DR, Downs DM, Cooper AJL, Fiehn O, Mullen RT, et al. (2014) Arabidopsis and Maize RidA Proteins Preempt Reactive Enamine/Imine Damage to Branched-Chain Amino Acid Biosynthesis in Plastids[C][W][OPEN]. Plant Cell 26:3010–3022.

11. Bussolati G, Geuna M, Bussolati B, Millesimo M, Botta M, Bartorelli A (1997) Cytolytic and tumor inhibitory antibodies against UK114 protein in the sera of cancer patients. Int. J. Oncol. 10:779–785.

12. Lambrecht JA, Flynn JM, Downs DM (2012) Conserved YjgF protein family deaminates reactive enamine/imine intermediates of pyridoxal 5’-phosphate (PLP)-dependent enzyme reactions. J. Biol. Chem. 287:3454–3461.

13. Degani G, Barbiroli A, Regazzoni L, Popolo L, Vanoni MA (2018) Imine Deaminase Activity and Conformational Stability of UK114, the Mammalian Member of the Rid Protein Family Active in Amino Acid Metabolism. Int. J. Mol. Sci. 19:E945.

14. Deriu D, Briand C, Mistiniene E, Naktinis V, Grütter MG (2003) Structure and oligomeric state of the mammalian tumour-associated antigen UK114. Acta Crystallogr. D Biol. Crystallogr. 59:1676–1678.

15. Liu X, Zeng J, Chen X, Xie W (2016) Crystal structures of RidA, an important enzyme for the prevention of toxic side products. Sci. Rep. 6:30494.

16. Burman JD, Stevenson CEM, Sawers RG, Lawson DM (2007) The crystal structure of Escherichia coli TdcF, a member of the highly conserved YjgF/YER057c/UK114 family. BMC Struct. Biol. 7:30.

17. Sinha S, Rappu P, Lange SC, Mäntsälä P, Zalkin H, Smith JL (1999) Crystal structure of Bacillus subtilis YabJ, a purine regulatory protein and member of the highly conserved YjgF family. Proc. Natl. Acad. Sci. U. S. A. 96:13074–13079.

18. Mistiniene E, Pozdniakovaite N, Popendikyte V, Naktinis V (2005) Structure-based ligand binding sites of protein p14.5, a member of protein family YER057c/YIL051c/YjgF. Int. J. Biol. Macromol. 37:61–68.

19. ElRamlawy KG, Fujimura T, Baba K, Kim JW, Kawamoto C, Isobe T, Abe T, Hodge-Hanson K, Downs DM, Refaat IH, et al. (2016) Der f 34, a Novel Major House Dust Mite Allergen Belonging to a Highly Conserved Rid/YjgF/YER057c/UK114 Family of Imine Deaminases. J. Biol. Chem. 291:21607–21615.

20. Siculella L, Giannotti L, Di Chiara Stanca B, Calcagnile M, Rochira A, Stanca E, Alifano P, Damiano F (2021) Evidence for a Negative Correlation between Human Reactive Enamine-Imine Intermediate Deaminase A (RIDA) Activity and Cell Proliferation Rate: Role of Lysine Succinylation of RIDA. Int. J. Mol. Sci. 22:3804.

21. Kanouchi H, Oka T, Asagi K, Tachibana H, Yamada K (2000) Expression and cellular distribution of perchloric acid-soluble protein is dependent on the cell-proliferating states of NRK-52E cells. Cell. Mol. Life Sci. CMLS 57:1103–1108.

22. Kanouchi H, Taga M, Okamoto T, Yamasaki M, Oka T, Yamada K, Tone S, Minatogawa Y (2006) Reduced expression of perchloric acid-soluble protein after partial hepatectomy in rats. Biosci. Biotechnol. Biochem. 70:290–292.

23. Asagi K, Oka T, Arao K, Suzuki I, Thakur MK, Izumi K, Natori Y (1998) Purification, characterization and differentiation-dependent expression of a perchloric acid soluble protein from rat kidney. Nephron 79:80–90.

24. Ceciliani F, Biancardi C, Cavalca V, Ferrara R, Botta M, Bailo M, Arzani C, Berra B, Ronchi S, Bartorelli A (1996) Structural characterization of the small molecular weight proteins present in UK101. J. Tumor Marker Oncol. 11:63–66.

25. Digiovanni S, Visentin C, Degani G, Barbiroli A, Chiara M, Regazzoni L, Di Pisa F, Borchert AJ, Downs DM, Ricagno S, et al. (2020) Two novel fish paralogs provide insights into the Rid family of imine deaminases active in pre-empting enamine/imine metabolic damage. Sci. Rep. 10:10135.

26. Madeira F, Park YM, Lee J, Buso N, Gur T, Madhusoodanan N, Basutkar P, Tivey ARN, Potter SC, Finn RD, et al. (2019) The EMBL-EBI search and sequence analysis tools APIs in 2019. Nucleic Acids Res. 47:W636–W641.

27. Robert X, Gouet P (2014) Deciphering key features in protein structures with the new ENDscript server. Nucleic Acids Res. 42:W320–W324.

28. Kelly SM, Jess TJ, Price NC (2005) How to study proteins by circular dichroism. Biochim. Biophys. Acta 1751:119–139.

29. Visentin C, Rizzi G, Degani G, Digiovanni S, Robecchi G, Barbiroli A, Popolo L, Vanoni MA, Ricagno S (2022) Apis mellifera RidA, a novel member of the canonical YigF/YER057c/UK114 imine deiminase superfamily of enzymes pre-empting metabolic damage. Biochem. Biophys. Res. Commun. 616:70–75.

30. Digiovanni S, Degani G, Popolo L, Vanoni MA Using d- and l-Amino Acid Oxidases to Generate the Imino Acid Substrate to Measure the Activity of the Novel Rid (Enamine/Imine Deaminase) Class of Enzymes. In: Barile M, editor. Flavins and Flavoproteins: Methods and Protocols. Methods in Molecular Biology. New York, NY: Springer US; 2021. pp. 199–218. Available from: https://doi.org/10.1007/978-1-0716-1286-6_13

31. Vagin A, Teplyakov A (2010) Molecular replacement with MOLREP. Acta Crystallogr. D Biol. Crystallogr. 66:22–25.

32. Emsley P, Cowtan K (2004) Coot: model-building tools for molecular graphics. Acta Crystallogr. D Biol. Crystallogr. 60:2126–2132.

33. Afonine PV, Grosse-Kunstleve RW, Echols N, Headd JJ, Moriarty NW, Mustyakimov M, Terwilliger TC, Urzhumtsev A, Zwart PH, Adams PD (2012) Towards automated crystallographic structure refinement with phenix.refine. Acta Crystallogr. D Biol. Crystallogr. 68:352–367.

34. Chen P-Y, Chang W-SW, Chou R-H, Lai Y-K, Lin S-C, Chi C-Y, Wu C-W (2007) Two non-homologous brain diseases-related genes, SERPINI1 and PDCD10, are tightly linked by an asymmetric bidirectional promoter in an evolutionarily conserved manner. BMC Mol. Biol. 8:2.

35. McNicholas S, Potterton E, Wilson KS, Noble MEM (2011) Presenting your structures: the CCP4mg molecular-graphics software. Acta Crystallogr. D Biol. Crystallogr. 67:386–394.

36. Gasteiger E, Hoogland C, Gattiker A, Duvaud S, Wilkins MR, Appel RD, Bairoch A Protein Identification and Analysis Tools on the ExPASy Server. In: Walker JM, editor. The Proteomics Protocols Handbook. Totowa, NJ: Humana Press; 2005. pp. 571–607. Available from: http://link.springer.com/10.1385/1-59259-890-0:571

TABLES

Table 1. Molecular mass and T_m of RidA variants.

$_{Ch}$RidA variant	Theoretical Molecular Mass (kDa)*		Experimentally derived Molecular Mass (kDa)	T_m (°C)	T_m in 4M urea (°C)
	Monomer	Trimer			
$_{Ch}$RidA	14.6	43.8	41.4	> 98	94
$_{Ch}$RidA-R107A	14.5	43.5	40.8	> 98	> 98
$_{Ch}$RidA-R107K	14.5	43.5	39.8	> 98	> 98
$_{Ch}$RidA-R107W	14.6	43.8	40.5	> 98	> 98
$_{Ch}$RidA-K78A	14.5	43.5	39.3	> 98	> 98
$_{Ch}$RidA-E124A	14.5	43.5	40.7	> 98	82.3
$_{Ch}$RidA-V25W	14.7	44.1	40.7	70	44
$_{Ch}$RidA-A108D	14.6	43.8	40.1	87	92.2
$_{Ch}$RidA-I126Y	14.6	43.8	41.4	86	83
$_{Hs}$Rida	14.8	44.4	42.3	>98	76
$_{At}$RidA-68S	13.1	36.3	34.2	82	36

*Theoretical Molecular Mass was estimated using ProtParam[36].

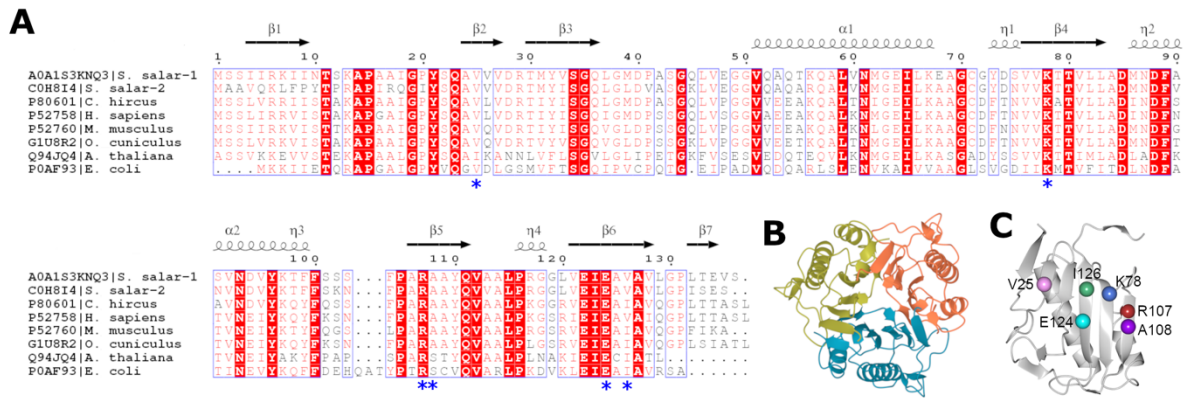

Figure 1. (A) Multiple alignment of RidA protein sequences from *S. salar-isoform1* (A0A1S3KNQ3), *S. salar-isoform 2* (C0H8I4), *C. hircus* (P80601), *H. sapiens* (P52758), *M. musculus* (P52760), *O. cuniculus* (G1U8R2), *A. thaliana* (Q94JQ4) and *E. coli* (P0AF93). Protein sequences were analysed using Clustal Omega and ESPript3. Fully conserved residues are highlighted in red; partially conserved residues are in red; blue frames indicate sequence stretches with globally high similarity. Blue stars indicate residues that have been mutated. The N-terminal signal peptide sequence of *A. thaliana* was omitted from the alignment. **(B-C)** Ribbon representation of $_{Ch}$RidA homotrimeric structure (PDB ID: 1NQ3) (B) and of a $_{Ch}$RidA monomer with residues mutated in this study shown as spheres (C).

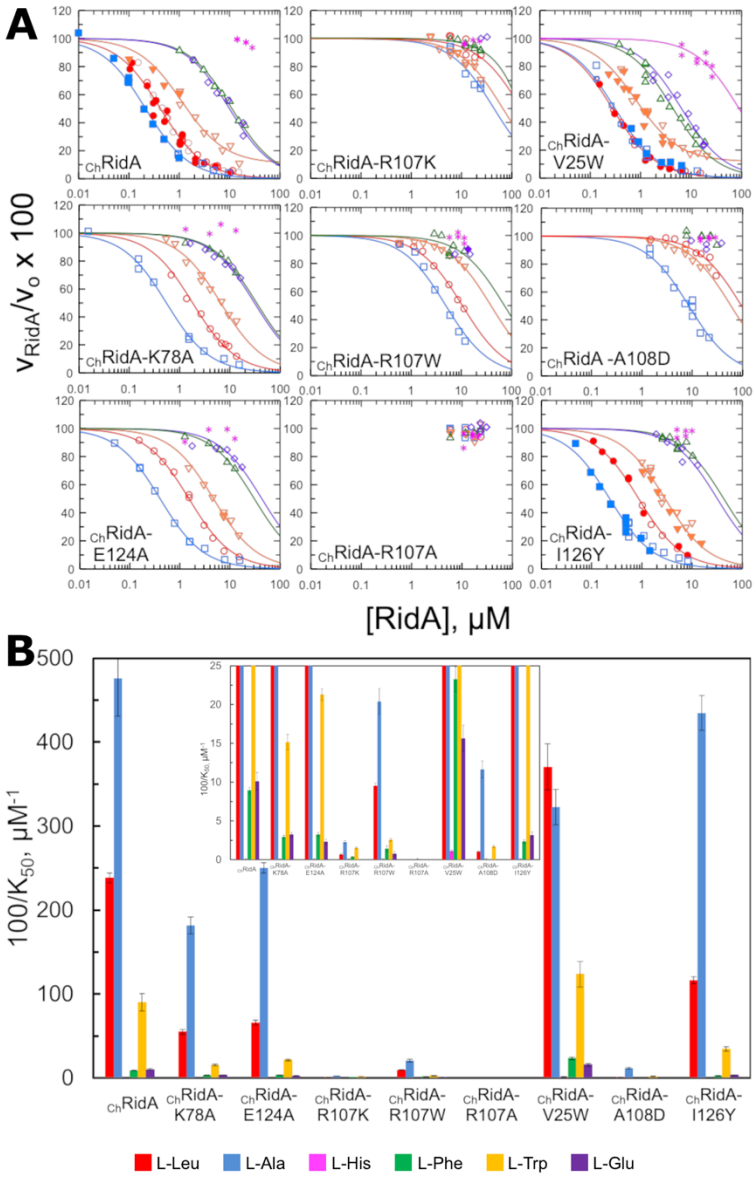

Figure 2. **Summary of the effects of amino acid substitutions on the substrate specificity of the RidA forms.**

(A) The activity of RidA variants, as measured from the initial velocity of semicarbazone formation in coupled assays containing different L-amino acids, LAAO, semicarbazide and varying amounts of RidA forms (v_{RidA}), is expressed as percentage of the initial velocity of semicarbazone formation in the absence of RidA (v_o). Symbols and colour code are as follows: L-Leu, red circles; L-Ala, blue squares; L-His, magenta stars; L-Phe, green triangles; L-Trp, orange inverted triangles; L-Glu, purple diamonds. Full symbols and empty symbols of different sizes indicate independent experiments. No curves were drawn when the RidA

variant had no detectable activity. (B) Catalytic efficiency of each RidA variant ($100/K_{50}$) with respect to the imino acids derived from six L-amino acids. The inset panel allows to inspect the low activity values exhibited by some of the RidA variants. Only V25W exhibited detectable activity with the imino acid derived from L-His.

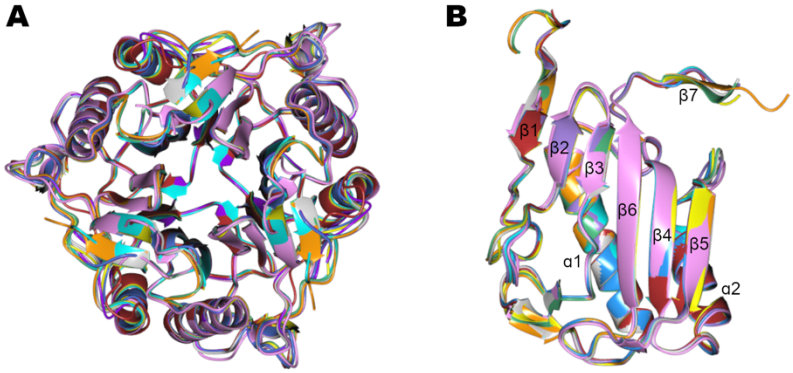

Figure 3. (A) Ribbon representation of the superposition of wt and mutant $_{Ch}$RidA trimers. Color code: Wt $_{Ch}$RidA, grey; $_{Ch}$RidA-R107A, red; $_{Ch}$RidA-R107K, orange; $_{Ch}$RidA-R107W, yellow; $_{Ch}$RidA-K78A, blue; $_{Ch}$RidA-E124A, cyan; $_{Ch}$RidA-V25W, pink; $_{Ch}$RidA-A108D, purple; $_{Ch}$RidA-I126Y, green. **(B)** Ribbon representation of the superposition of wt and variant $_{Ch}$RidA monomers using the same color code as in A.

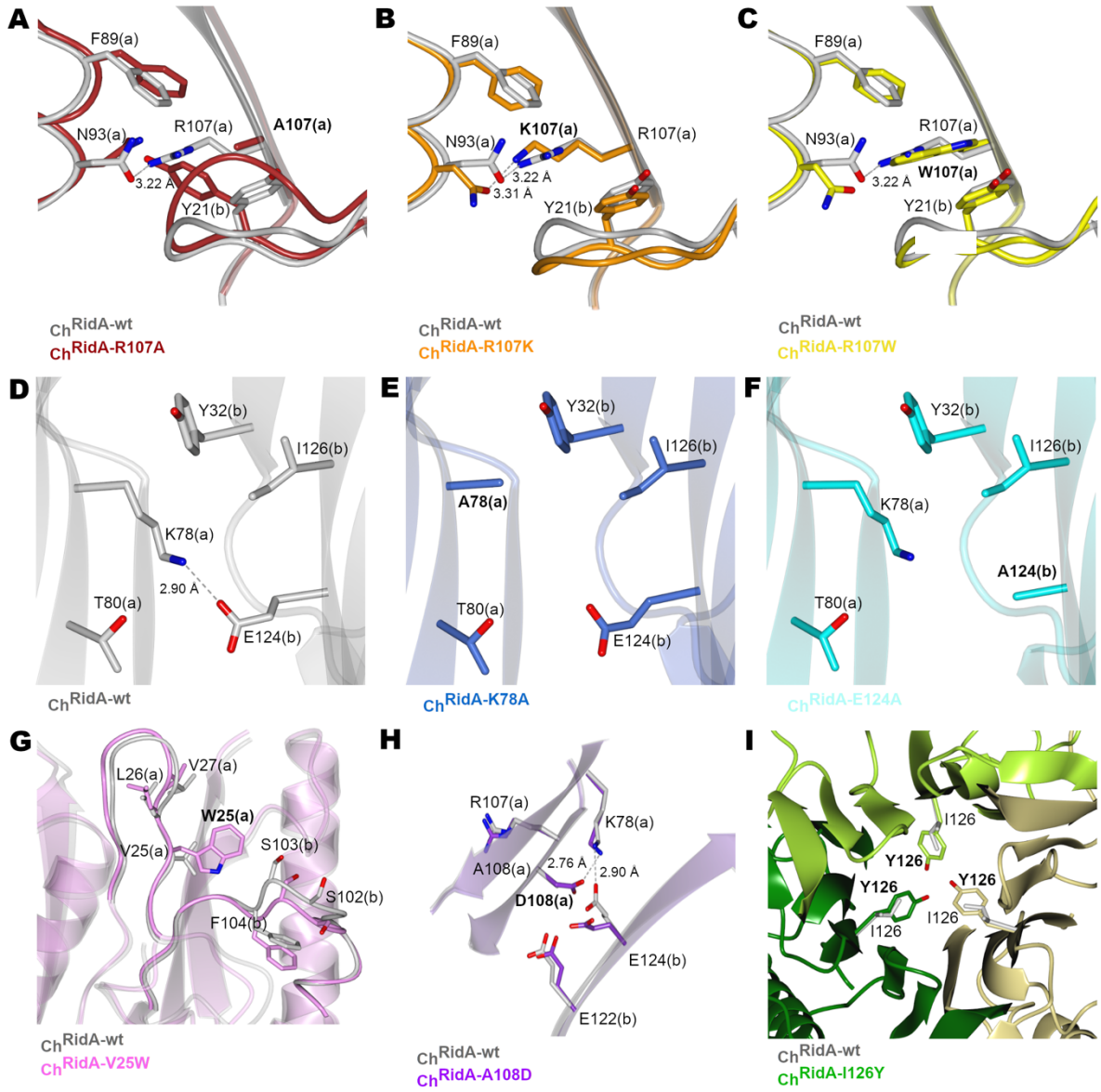

Figure 4. (A-C) Representation of active site of $_{Ch}$RidA-R107A (red, A), $_{Ch}$RidA-R107K (orange, B) and $_{Ch}$RidA-R107W (yellow, C) in comparison with wt $_{Ch}$RidA. Dotted lines represent the interatomic distances between atoms. **(D-F)** Representation of the inter-monomeric interface of wt $_{Ch}$RidA (grey, D), $_{Ch}$RidA-K78A (blue, E), and $_{Ch}$RidA-E124A (light blue, F). The salt bridge present in wt $_{Ch}$RidA is represented as dotted line. **(G)** Comparison of residues orientation of $_{Ch}$RidA-V25W (pink) and wt $_{Ch}$RidA (grey) in the proximity of V25W mutation. **(H)** Comparison of residues orientation of $_{Ch}$RidA-A108D (purple) and wt $_{Ch}$RidA (grey) in the proximity of A108D mutation. Salt bridges are

represented as dotted lines. **(I)** Comparison of residues orientation and central cavity filling of $_{Ch}$RidA-I126Y (green) and wt $_{Ch}$RidA (grey). In $_{Ch}$RidA-I126Y the three monomers are represented with different shades of green.